Materials and Design 117 (2017) 316–325

Contents lists available at ScienceDirect

Materials and Design

journal homepage: www.elsevier.com/locate/matdes

The limitations of electrical resistance for accurate positioning of shape-memory actuators: The case of well-oriented CuZnAl single-crystals under uniaxial loading

G. Bertolino *, A. Yawny, J.L. Pelegrina

Centro Atómico Bariloche, CNEA, R8402AGP San Carlos de Bariloche, Argentina
Instituto Balseiro, CNEA, Universidad Nacional de Cuyo, Argentina
CONICET, Argentina

HIGHLIGHTS

- The use of electrical resistance as a feedback signal for positioning of shape memory based actuators is critically revised.
- A physics-based model relating electrical resistance variation with strain for a single crystal benchmark case is presented.
- Even in the simplest case, a straightforward accurate correlation between strain and electrical resistance does not exist.
- Guidelines for selection of a shape memory material for actuator positioned through the electrical resistance are formulated.

GRAPHICAL ABSTRACT

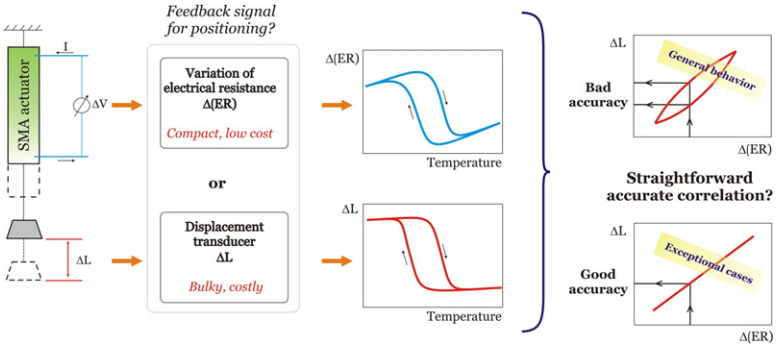

ARTICLE INFO

Article history:
Received 25 October 2016
Received in revised form 1 December 2016
Accepted 2 January 2017
Available online 3 January 2017

Keywords:
Martensitic transformations
Electrical resistance
Actuators
Positioning

ABSTRACT

The possibility of using the electrical resistance as a feedback signal for precise positioning in the design of compact shape-memory actuators was revised. The analysis was performed on well-oriented CuZnAl single crystalline shape-memory alloys subjected to uniaxial tensile loadings, combining direct strain measurements determined with an extensometer and the four-lead electrical resistance technique. In that way the relationship between strain and electrical resistance could be evaluated by formulating a physics based model that can be easily contrasted with the experimental characterization of a simple benchmark system. It was found that the model here developed provides general guidelines for the selection of a shape-memory material for positioning actuators and that the correlation between strain and electrical resistance is of rather limited precision, even for the simplest material case and loading condition analyzed. The effects of temperature, deformation rate, temperature dependence of the electrical resistivity of austenite and martensite phases and temperature dependence of the strain associated with the stress induced transformation were carefully characterized. Results suggest that the direct use of feedback from electrical resistance measurements for precise positioning is arguable unless materials with low hysteresis and low latent heat of transformation are used in combination with quasi-static operating conditions.

* Corresponding author at: Centro Atómico Bariloche, CNEA, R8402AGP San Carlos de Bariloche, Argentina.
E-mail address: bertolin@cab.cnea.gov.ar (G. Bertolino).

http://dx.doi.org/10.1016/j.matdes.2017.01.002
0264-1275/

1. Introduction

Shape Memory Alloys (SMA) belong to a special class of materials exhibiting particular behavior in the stress-strain-temperature space. Responsible for these effects in these materials is the existence of a nearly reversible stress induced martensitic phase transformation between an austenitic and a martensitic phase. This solid to solid first order phase transformation can be induced either thermally or mechanically. In the first case, austenite, which is the stable phase at the higher temperatures, begins to transform into martensite at a characteristic temperature referred to as M_S (martensite start temperature) upon cooling. The volume fraction of martensite increases progressively while cooling is continued until the temperature M_F (martensite finish) is reached where the specimen is completely transformed. Upon heating from below M_F, the reverse transformation occurs in the temperature interval between A_S and A_F (austenite start and finish temperatures, respectively). The precise relative position between these characteristic temperatures depends on the particular SMA system considered, being always the case that $A_F > M_S$. A hysteresis characterizing the thermally induced transformation can be defined as the difference $\Delta T = A_F - M_S$ [1].

Due to the complexity of the overall thermomechanical response exhibited by SMA, some particular trajectories in the stress-strain-space are usually taken to describe their behavior [2]. The so called one way shape memory effect, that gives the name to these alloys, is one of them. Superelasticity, also known as pseudoelasticity, is another of the distinguishing effects exhibited by SMA. It is the capacity exhibited by these materials to deform under the application of a mechanical load and at a certain constant temperature to a strain of approximately 10% in a nearly reversible manner. In superelasticity, the solid to solid phase change starts taking place in the forward direction from austenite to martensite once a critical stress σ_C^F is reached. Upon unloading, the transformation reverts, but this occurs at a stress σ_C^R, lower than σ_C^F, which gives rise to a mechanical hysteresis defined as $\Delta\sigma = \sigma_C^F - \sigma_C^R$. The original specimen dimensions are recovered in this way.

The critical stresses are related with temperature T (and vice versa) according to a Clausius-Clapeyron type of relation which gives the slope $r_\sigma = d\sigma_C/dT = -\Delta S_{tr}/\varepsilon_{tr}$ in terms of the entropy change ΔS_{tr} and the strain change ε_{tr} associated with the transformation between austenite and martensite [3]. The temperature dependence of the critical stresses can be determined experimentally with typical values ranging from 6 to 7 MPa/°C for NiTi SMA [4] and 2 MPa/°C for well oriented Cu-based single crystals [5]. This coupling between temperature and critical transformation stress results in a dependence of the mechanical response on the strain rate, the ambient temperature and the heat transfer characteristics between specimen and surroundings [4,6].

From the point of view of the practical use of SMA, applications can be classified as those based on the superelastic effect (stents, orthodontic wires, damping devices), those combining the one way shape memory effect and the constrained recovery (couplings, liberation systems) and the application in actuators where a SMA nucleus can perform work against a certain force by controlling its temperature [2,7,8]. In that way, a temperature variation induces a dimensional change that can be used for accurate positioning in micromechanisms. To avoid the use of bulky and expensive displacement sensors, the electrical resistance variation of the SMA actuator element has been considered for providing an alternative feedback control variable instead of directly using the elongation value measured with a conventional transducer, e.g., with an LVDT (Linear Variable Differential Transformer) [9]. This proposal is based on the potential relationship between the proportion of phases and the global elongation of the SMA transforming specimen. Actually, the variations of electrical resistance during transformations had motivated a series of studies both from basic and applied perspectives. In the former case, the variations of electrical resistance were used to infer about the material evolutions associated with the thermally or stress induced martensitic transformations, e.g. [10,11], while in the latter case the efforts were devoted to explore the possibility of finding a unique correspondence between the electrical resistance variation and the deformation of the specimen. With this purpose, intensive studies to characterize the relation between strain and electrical resistance variation in NiTi and Cu-based SMA can be found in the literature [12–22]. In spite of these efforts, the results are still inconclusive mainly due to the complexities associated with the non-linear behavior exhibited by SMA, the presence of a hysteresis and the latent heat associated with the first order martensitic transformation responsible of the singular behavior of these materials and whose effects are very often completely ignored in spite of their definite role as will be shown later in the present study.

The persistence of these limitations can be clearly appreciated by analyzing the most recent literature on the matter. Lynch et al. [19], considered taking as valid only the linear portions of the more complex relationship between strain and electrical resistance found in their work (Fig. 5 therein). Analysis of Fig. 11 in Cho et al. [20] indicates that discrepancies of nearly 30% between calculations and modeling were obtained and considered however acceptable. Other authors [21, 22] have proposed complex models based on a certain number of adjustable parameters having no clear identification or relationship with properties of the specific SMA material and the martensitic associated transformation responsible of the actuation effect.

The main purpose of the present work is to analyze the possibility of using the electrical resistance as a feedback signal for positioning of SMA actuators. It is expected that general guidelines for the design and for the selection of an appropriate SMA material can be provided. In order to get insight on fundamental limitations, the simplest system available to the present authors was selected for the analysis. CuZnAl single crystalline shape memory alloys subjected to uniaxial tensile loadings will be considered to formulate a simple model for electrical resistance variation that can be contrasted with an appropriate experimental characterization. In that way, complex contributions arising from grain boundaries and interfaces between martensite variants with different orientations are eliminated. It is expected that the analysis here performed allows defining a benchmark case against which the behavior of more complex systems can be compared.

2. A basic model to understand the principle of positioning using electrical resistance

As a first step in formulating a basic model to understand the relationship between electrical resistance change and the associated strain of a shape memory material specimen, the idealized pseudoelastic behavior represented in Fig. 1 will be assumed. Therein, the only contributions to the strain and to the electrical resistance variations are considered to be due to the stress induced transformation. To which extent these assumptions are reasonable will be object of analysis in further sections.

Fig. 1 illustrates five stages associated with the progression of the pseudoelastic transformation of a specimen which is initially in the austenite phase having a length L_A. By imposing a progressively increasing displacement ΔL, an increasing amount of material will forward transform to martensite at a critical stress σ_C^F corresponding to the temperature T_1 ($T_1 > A_F$). The maximum attainable strain is given by ε_{tr} which corresponds to the crystallographic uniaxial strain associated with the stress induced transformation.

The current length L of such partially transformed specimen will depend on the volume fraction of the austenite that has been transformed into martensite by the imposed deformation. As only ideal thermoelastic transformations are dealt with in this work, the associated volume change between the phases involved is considered to be negligible [23]. Therefore, the transformed volume fraction is equivalent to the transformed length fraction, referred to as f in the present work. Thus the length L can be expressed as

$$L = (1-f)\, L_A + f\, L_M \tag{1}$$

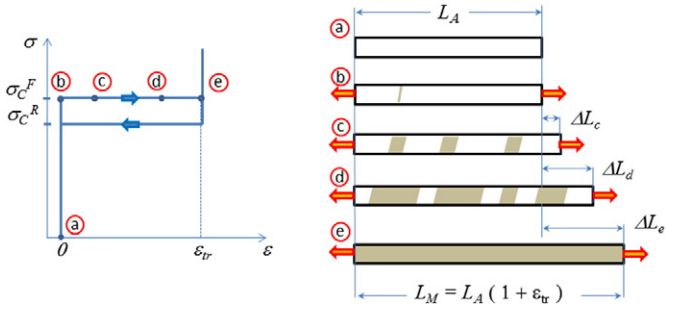

Fig. 1. Idealized transformation model at constant temperature $T_1 > A_f$. Point a corresponds to the unloaded austenite phase. Point *b* corresponds to the incipient nucleation of a martensite domain at the critical stress σ_C^F. Further imposed increasing displacements ΔL_c, ΔL_d results in the progressive increase of the fraction of transformed material (points *c* and *d*) until ΔL_e is reached where the specimen is fully transformed (point *e*).

that can be written in the more compact form

$$L = L_A\,(1 + f\,\varepsilon_{tr}) \tag{2}$$

The corresponding global macroscopic strain of the specimen ε that can be determined experimentally by measuring the variation of the total length of the specimen would be given by

$$\varepsilon = \frac{\Delta L}{L_A} = \frac{(L - L_A)}{L_A} = f\,\varepsilon_{tr} \tag{3}$$

For a fully transformed specimen $f = 1$, thus $L = L_M = L_A\,(1 + \varepsilon_{tr})$ and $\varepsilon = \varepsilon_{tr}$. If S_A is the cross-section area of the austenite specimen, the cross-section area S_M of the portions that have transformed to martensite can be easily calculated considering the constancy of volume condition as

$$S_M = \frac{S_A}{1 + \varepsilon_{tr}} \tag{4}$$

On the other hand, the global electrical resistance R of the specimen can be also estimated by a simple rule of mixtures considering that the austenite and martensite domains are disposed in series and assuming a negligible influence of the interfaces between them, i.e.

$$R = (1 - f)\,R_A + f\,R_M \tag{5}$$

where $R_A = \rho_A\,L_A/S_A$ and $R_M = \rho_M\,L_M/S_M$ are the corresponding electrical resistances of the specimen fully in austenite and fully in martensite, with ρ_A and ρ_M the electrical resistivity of the austenitic and martensitic phases, respectively. After introducing the dimensionless variable $R^* = (R - R_A)/R_A$, Eq. (5) can be expressed as

$$R^* = \frac{\varepsilon}{\varepsilon_{tr}}\left(\frac{R_M - R_A}{R_A}\right) \tag{6}$$

or as

$$R^* = \frac{\varepsilon}{\varepsilon_{tr}}\left[\frac{\rho_M}{\rho_A}\,(1 + \varepsilon_{tr})^2 - 1\right] \tag{7}$$

Analysis of Eqs. (6) or (7) indicates that the simple isothermal model here assumed predicts a linear relationship between the change in electrical resistance and the global strain of the specimen. As the electrical resistivity of the individual phases might have a different dependence with temperature, and also the magnitude of ε_{tr} might depend on temperature, the proportionality between electrical resistance and strain would also depend on the particular temperature considered. If the whole relationship between R and ε is desired, the temperature dependence of the electrical resistance should have been taken into account. The relationship for the non-isothermal case is presented in Appendix A.

This observation is particularly relevant in the case of positioning applications or in actuators based on shape memory materials, where the actuation is promoted precisely by changing the temperature of the SMA actuator nucleus. Therefore, strictly isothermal situations seldom, if ever, occur in practice. In effect, real actuators are also subjected to variable loads of different origins, and variable loads in turn require changing the temperature of the shape memory material, according to the Clausius-Clapeyron relationship, for actuation. On the other hand, shape memory alloys exhibit different degrees of temperature hysteresis which introduces necessary temperature variations in case of reversing the actuation direction. For the pseudoelastic isothermal idealized cycle shown in Fig. 1, the mechanical hysteresis given by the difference $\Delta\sigma = \sigma_C^F - \sigma_C^R$ will have a corresponding thermal hysteresis in a constant stress situation given by $\Delta T = \Delta\sigma/r_\sigma$ (more quantitative details will be given in the next sections). Additionally, it should be recalled that martensitic transformations are first order solid to solid phase transformations and thus they involve a latent heat of transformation. This heat results in changes in the temperature of the transforming specimen, being the magnitude of the temperature variation dependent on the speed of actuation due to heat transfer considerations. The just mentioned factors imply that direct use of the relationship between the electrical resistance variation and the global strain established by Eq. (7) might not be straightforward, i.e., the temperature variations might be affecting the positioning accuracy.

In spite of the just mentioned limitations, the previous analysis provides an important first basic criterion when seeking for a shape memory material for actuator applications where electrical resistance changes can be used to control positioning. From this point of view, a low stress dependence of the critical transformation temperatures and a low temperature hysteresis is recommendable. Based on these considerations it can be concluded that, NiTi is a better alternative compared with Cu-based SMA when considering the first aspect. In effect, it shifts approximately 0.14 °C/MPa ($r_\sigma \approx 7$ MPa/°C) compared to 0.5 °C/MPa ($r_\sigma \approx 2$ MPa/°C) for well oriented Cu-based single crystals, value that can be even higher in the case of polycrystalline specimens. On the other hand, a thermal hysteresis of 30 °C puts NiTi in disadvantage against the 1 °C to 2 °C hysteresis exhibited by single crystalline Cu-based SMA.

It is important to remark that even when at a first sight the model presented here might seem simplistic in extreme, it could describe the behavior of well oriented Cu-based SMA single crystals where most of the basic assumptions that have been adopted find close correspondence. In the case of certain NiTi alloys where the transformation from austenite to martensite is preceded by R-phase formation [24,25], the simple model presented here must be reformulated. Based on the previous considerations, experiments in single crystalline Cu-based material will be performed to investigate on the feasibility of using electrical resistance measurements for accurate positioning in SMA actuation. Also in a further section, the different factors that were disregarded in the formulation of the model and that might be attempting against the extension of the linear dependency to a wide temperature range will be analyzed.

3. Experimental details

The experiments performed in the present work pointed to evaluate the electrical resistance changes of Cu-Zn-Al single-crystalline specimens subjected to simultaneous deformation due to a stress or a temperature induced martensitic transformation. Details about the specimen preparation and on the techniques employed are provided in what follows.

A Cu - 14.35 Zn - 16.83 Al (at%) alloy with a nominal martensitic transformation start temperature M_S of −4 °C has been prepared by melting 99.99% pure metals in sealed quartz tubes under Ar atmosphere. Two cylindrical single crystals, SXA and SXB, 6 mm in diameter and 14 cm in length were grown by the Bridgman method, also using

sealed quartz tubes and Ar atmosphere. The orientation of the crystals was determined using the X-ray Laue technique. The longitudinal axis of crystal SXA resulted in [1 10 14] while of crystal SXB in [1 13 21]. From each of the crystals, a cylindrical tensile specimen with axis parallel to the crystal axis was obtained by spark-erosion. They will be referred to as specimens A and B. Their respective Schmid factor, m, for the calculation of the resolved shear stresses τ from the applied stresses σ, resulted in $m = 0.421$ and 0.444 ($\tau = m\,\sigma$). Tensile specimen A was spark-machined to the double dog-bone shape represented in Fig. 2, with a 12 mm central part 2 mm in diameter, followed by 10 mm long 3 mm in diameter segments and the heads for hanging type griping. Specimen B was spark-machined to a simple dog-bone shape with a central 30 mm long 2.7 mm reduced diameter with the same type of heads. The geometry of specimen A ensured that all transformation activity was restricted to the gauge length of the extensometer because the nucleation and growth of the martensite plates occurred within the 2 mm diameter zone. On the other hand, the simpler geometry of specimen B enabled an easier interpretation of the strain and electrical resistance measurements. The specimens were homogenized at 800 °C for 900 s followed by quenching in water at room temperature (i.e., above M_S) and they were kept at least one week in the austenite phase prior to testing.

The tests were performed in an Instron 5567 electromechanical testing machine equipped with a temperature chamber Instron 3119-005 using the set-up illustrated in Fig. 2. The four-lead technique was used for electrical resistance measurement. For that, Cu cables were spot welded at the positions shown in the figure. A direct current of 200 mA was injected through cables welded to the specimen heads. The sense of the current was inverted in order to discard the effect of temperature gradients in the specimen. The corresponding voltage drop, measured using an Agilent 34420A nanovoltmeter, was obtained as one half the difference of the values from both possible current directions. The temperature was followed using a Chromel-Alumel thermocouple (T.C.) attached to one of the grips close to the specimen head contact zone. The axial strain was assessed using an axial clip-on extensometer Instron 2620-602 with a gauge length of 25 mm affixed to the central part of the specimen.

Pseudoelastic cycles were performed under constant crosshead displacement rate conditions. Different temperatures and speeds were selected according to the test purpose and the specific values will be provided elsewhere in the Results and discussion section. The maximum imposed strain in the cycles was determined by the appearance of an increase in the plateau slope to ensure full transformation to stress induced martensite in the region of interest.

Additional experiments to evaluate the electrical resistance variation corresponding to temperature induced transformations under an applied constant load have been performed. They were conducted under load control and the temperature was varied using the temperature chamber in order to fully transform the specimen, forth and back between the austenitic and martensitic phases.

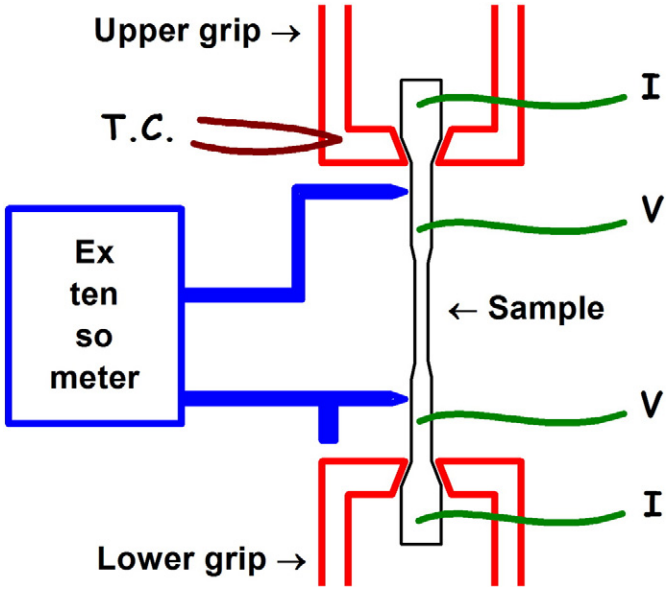

Fig. 2. Schematic of the experimental set-up used for the simultaneous measurement of electrical resistance and strain during stress induced transformations in Cu-Zn-Al single crystals. Type A Specimen is illustrated.

4. Results and discussion

In this section the experimental results concerning the pseudoelastic response of the material employed will be presented first. This will be followed by the characterization of the associated electrical resistance variations and then by the relationship between the latter and the corresponding strain. The effects of temperature and strain rate will be evaluated in each case. Finally, the influence of different factors that has been ignored in the formulation of the simplified model previously presented will be discussed.

4.1. Experimental characterization of the pseudoelastic behavior

Fig. 3a shows the pseudoelastic behavior of specimen A obtained at four different temperatures (24 °C, 50 °C, 75 °C and 100 °C) using a crosshead displacement rate of 2 mm/min. To facilitate further comparisons with specimen B, the cycles are represented in terms of the applied resolved shear stress τ, but the axial strain ε will be maintained for the comparison with R. It can be seen that in all cases the cycles exhibit a nearly horizontal region (*plateau*) followed by a zone where the slope increases gradually. The constant stress region corresponds to the transformation of the central reduced diameter section, while the inclined part can be associated to the transformation in the transition from the central zone and the contiguous increased diameter regions where the extensometer is attached (Fig. 2). The low slope of the stress-strain curve constitutes a clear indication that the main contribution to the strain measurement comes from the transformation of the remaining austenite instead from the elastic deformation of the martensite. It will be shown in Section 4.4 that, the electrical resistance is almost insensitive to the elastic deformation of the material, thus the effect of the elastic deformation can be discarded in the analysis of the results. The stress at which the transformation starts, usually known as the critical resolved shear stress $\tau_C^F = m\,\sigma_C^F$ follows the linear dependence with temperature shown in Fig. 3b. These cycles allow appreciating the singular characteristics associated with Cu-based single crystalline SMA, in particular the reduced value of the mechanical hysteresis given by the difference $\Delta\tau = \tau_C^F - \tau_C^R$, which, for example, at a reference strain of 1% reaches values of 3.4 MPa at 24 °C and 4.5 MPa at 100 °C. The resulting slope $r_\tau = d\tau_C^F/dT = (1.05 \pm 0.02)$ MPa/°C is independent of the particular orientation of the tensile axis of the sample [5]. This linear dependence extrapolates at zero stress to 0 °C, close to the alloy nominal transformation temperature M_S for a pure thermally induced transformation ($M_S = -4$ °C). It is important to remark here that such close correspondence between the M_S temperature and the extrapolated value of the linear fitting to zero stress is proper of Cu-based alloys and does not necessarily hold for commercial NiTi-ultrafine grained materials being used in technological applications nowadays (see for example [24]). The linear relationship extends into the high stress region until plastic deformation becomes operative.

The effect of the transformation rate on the pseudoelastic behavior was evaluated by performing cycles at different crosshead speeds in the range 0.1 to 2 mm/min at the four temperatures previously considered. Fig. 4a shows representative results of experiments performed at 50 °C. It can be seen that the increase in the transformation rate results in an increase (decrease) of the stress for the forward (reverse)

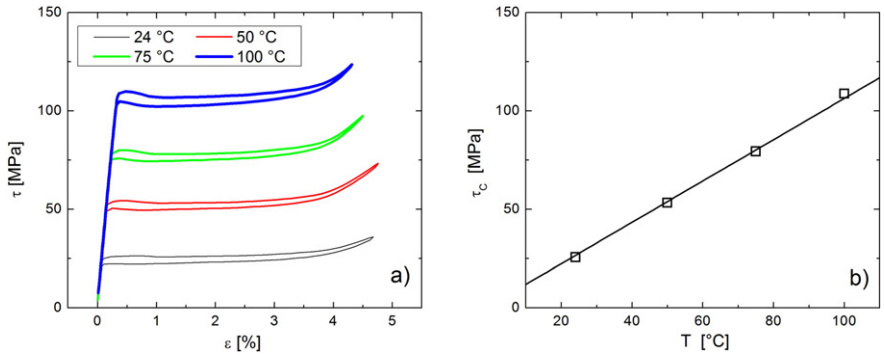

Fig. 3. Effect of temperature on the martensitic transformation. a) Pseudoelastic cycles at a crosshead speed of 2 mm/min. b) Clausius-Clapeyron relation. Specimen A.

transformation. The corresponding increments of the mechanical hysteresis $\Delta\tau_1$ determined at a strain of 1% are represented in Fig. 4b. The observed mechanical variations are consequence of the temperature changes induced in the specimen due to the latent heat of transformation. The forward transformation from austenite to martensite, being exothermic, results in an increase of the temperature in the zone where the stress induced transformation is taking place. Due to the dependence of the critical transformation stress with temperature, a consequent increase of the stress is produced as a response to the imposed transformation rate. The opposite occurs with the reverse transformation from martensite to austenite because of its endothermic character.

Analysis of Fig. 4b suggests an almost similar linear dependence of the thermal hysteresis with the crosshead speed for 24 °C, 50 °C and 75 °C. The data corresponding to 100 °C however, clearly departs from this common behavior. At this temperature, the increase of the mechanical hysteresis is more noticeable, being it even more marked at low speeds. To rationalize this effect it should be remembered here that Cu-based SMA are susceptible to the phenomenon of martensite stabilization [26]. This is an atomic diffusion mediated process that alters the stability of the martensite by the rearrangement of the atom distribution within the martensitic structure. As a consequence the martensite results thermodynamically stabilized with respect to austenite and there is an increase of the temperature for the reverse transformation of martensite or, equivalently, a decrease of the reverse transformation stress. Being atomic diffusion a temperature and time dependent phenomena, the effects of martensite stabilization are expected to be more significant the higher the temperature and the lower the transformation rate. This is evidenced in Fig. 4b by the decreasing slope observed in the curve corresponding to 100 °C at low speeds. These results suggest an operational upper temperature limit for CuZnAl SMA actuators. The limit however can be extended to higher temperatures in systems less prone to the phenomenon of martensite stabilization as are some CuAlBe and CuAlNi alloys.

It is worthwhile to remark here that the global behavior and the particular features associated with the pseudoelasticity that were described above are highly reproducible. This is an essential aspect in the context of the present work where the influence of the different factors affecting the relationship between electrical resistance and strain wants to be analyzed. This very good reproducibility is exemplified in Fig. 5 where three consecutive pseudoelastic cycles performed in specimen A at a crosshead speed of 2 mm/min are presented. It can be seen that the overlapping between the cycles in the whole elastic and transforming range is remarkable which provides confidence in the further assessments.

4.2. Experimental characterization of the electrical resistance variations during pseudoelastic cycling

The results concerning the variation of the electrical resistance associated with a pseudoelastic cycle are now presented. In Fig. 6a, the electrical resistance is plotted as a function of time for three consecutive pseudoelastic cycles performed in specimen A at 24 °C using a crosshead speed of 0.2 mm/min. It can be seen that a very good overlapping exists among the three electrical resistance vs. time curves which indicates a good reproducibility of the measurements, similarly to what has been observed before in Fig. 5 concerning the mechanical behavior. In Fig. 6b the mean value of the three electrical resistance curves shown in Fig. 6a is presented as a function of time, together with the corresponding variation of the resolved shear stress during the pseudoelastic cycle. It can be seen that the relevant changes observed in the electrical resistance are associated with the forward and reverse stress induced transformations. The variation of the electrical resistance occurring during

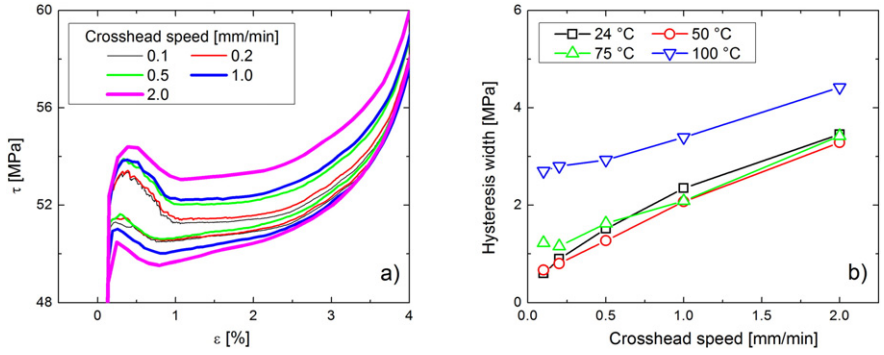

Fig. 4. a) Pseudoelastic cycles at different crosshead speeds at a fixed temperature of 50 °C. b) Dependence of the mechanical hysteresis $\Delta\tau_1$ determined at 1% strain with imposed crosshead speed at different temperatures. Specimen A.

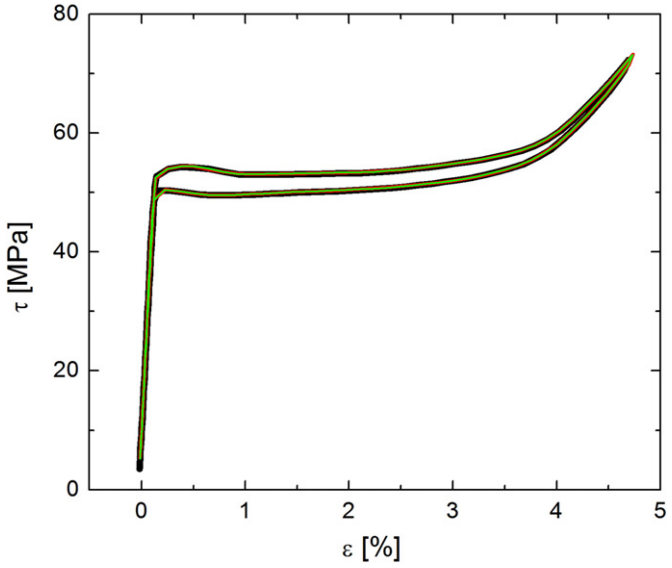

Fig. 5. Three consecutive pseudoelastic cycles performed at a crosshead speed of 2 mm/min and 50 °C. Specimen A.

the elastic loading and unloading parts of the pseudoelastic cycle are minor, in line with previous findings for other Cu-based-SMA [27] (the magnitude of the changes associated with the elastic components of the deformation will be quantitatively estimated in a next section). In effect, the marked increase observed in the slope of the electrical resistance vs. time plot is associated with the point in the stress vs. strain curve where the forward stress induced transformation starts. From this point on, the slope remains nearly constant up to maximum load is reached. One aspect deserving further clarification is the observation that the electrical resistance does not reach a constant value after the plateau region. This has to do with the particular geometry of specimen A used in the experiments because, as it was explained before, after the 2 mm in diameter central part is transformed, the stress induced transformation extends into the transition region with the 3 mm in diameter region where the cables used to measure the voltage difference are spot welded and the extensometer is attached. The linear behavior exhibited by the electrical resistance during transformation and the repeatability of the observed behavior was confirmed for all the temperatures used in the present work.

In Fig. 7a, the effect of the temperature on the variations of the electrical resistance during pseudoelastic cycles is illustrated. As the resistance of the austenite varies with temperature and in order to compare the results for the different experimental conditions, it was considered convenient to plot the dimensionless variable R^* as a function of time, as shown in Fig. 7b. As can be appreciated from the pseudoelastic cycles presented in Fig. 3a, an increase in temperature results in an increase of the transformation stresses. This in turn results in an increase of the extension of the elastic strain range during loading. As the same value of maximum strain was used in all cases, the contribution of the transformation to the total strain decreased with increasing temperature. Due to that, it would also be expected that the maximum value of R^* decreases with temperature. These two facts explain the particular relationship between the curves shown in Fig. 7b, i.e., the higher the temperature the lower the maximum in R^* and the shorter the extension of the electrical resistance variations associated with the stress induced transformation. The measured maximum variation of the dimensionless resistance at each temperature R^*_{MAX} was represented as a function of the associated maximum strain in Fig. 7c. It can be seen that a good correlation exists between both variables and that for the cycles performed at 24 °C and 50 °C that were conducted until a similar maximum strain, the variation of R^*_{MAX} coincides within experimental scatter, in spite of the temperature difference. Therefore, the dimensionless variable R^* seems to be significantly more sensitive to the strain associated with the transformation than to possible temperature variations.

The influence of the transformation rate on the electrical resistivity response is now analyzed. In order to facilitate the comparison of results corresponding to different crosshead speeds, results are plotted in terms of a normalized time value defined as t/t_T where t_T is the total time of crosshead movement plus two intervals for the reference state in the unloaded state, one at the beginning and the other at the end of the experiment. The behavior of R^* vs. t/t_T is presented in Fig. 8. It can be seen that once the transformation starts, the resistance R^* varies linearly, following the same path, independently of the deformation rate. These results confirm that R^* is significantly more sensitive to strain than to temperature changes introduced by the latent heat of transformation. This constitutes an important difference with the behavior observed for pseudoelasticity where both the critical stresses for transformation and the mechanical hysteresis were shown to exhibit a strong dependence with the deformation rate (see Fig. 4a and b).

4.3. Strain vs. electrical resistance

In Fig. 9 the experimental relationship between the strain and the corresponding variation of the electrical resistance is analyzed. The results obtained from two experiments performed at 50 °C using crosshead speeds of 0.2 mm/min and 2 mm/min are shown in Fig. 9a and b, respectively. They can be considered representative of the other temperature conditions used in the present work. For the transformation carried out at 0.2 mm/min, a linear behavior with superposed forward and reverse transformation branches is observed (Fig. 9a). For a factor ten increase of the deformation rate to 2 mm/min, the linearity and its slope are maintained but a separation between the forward and reverse transformation branches can be discerned (Fig. 9b), being it apparent that the associated R^* value is higher for the reverse transformation.

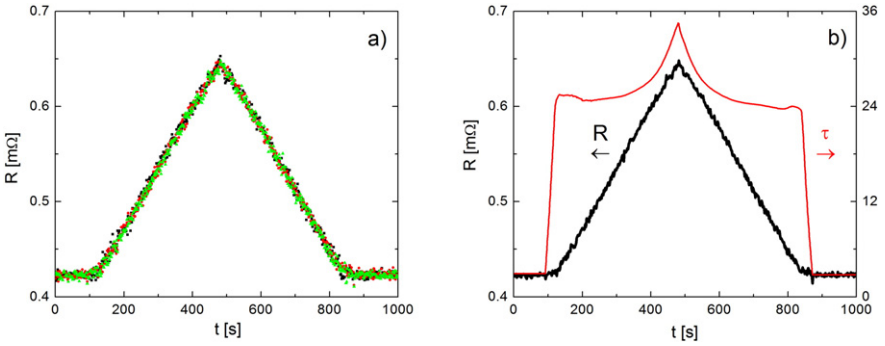

Fig. 6. a) The electrical resistance measured for three consecutive pseudoelastic cycles as a function of the time of the experiment, at a crosshead speed of 0.2 mm/min and 24 °C. b) Comparison between the mean electrical resistance evolution (thick line) and the applied stress (thin line). Specimen A.

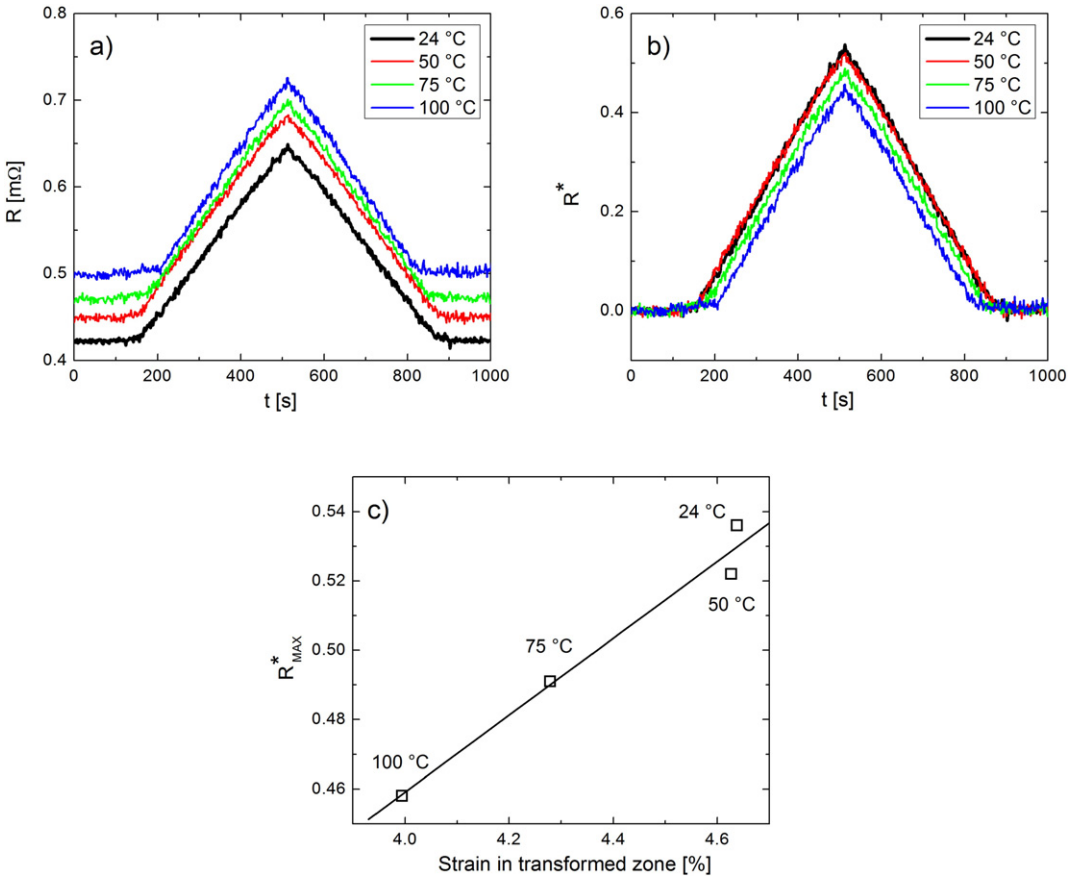

Fig. 7. a) Effect of temperature on the electrical resistance during the martensitic transformation at a crosshead speed of 0.2 mm/min. b) Electrical resistance variations of Fig. 7a presented using the dimensionless variable R^*. c) Maximum variation of the dimensionless electrical resistance as a function of the maximum strain reached at each temperature. Specimen A.

Recalling the independence with the transformation rate and the relationships between R^* and ε expressed in Eqs. (6) and (7), the mean values of the slopes for the five crosshead speeds are represented in Fig. 9c as a function of the test temperature. This slope $dR^*/d\varepsilon$ should correspond to the proportionality factor between both variables discussed before. The analysis of Fig. 9c indicates a temperature dependence of the slope value of nearly $0.07\%/^{0}C$, suggesting that care should be taken in assuming that ε could be reasonably assessed by experimentally determining R^*. The mean value of $dR^*/d\varepsilon \sim 11$ taken from the values plotted in Fig. 9c and a typical scatter of $\Delta R^* = 0.006$ from the present electrical resistance measurements enable in principle the determination of the strain with an uncertainty of $\Delta\varepsilon = 0.0006 = 0.06\%$.

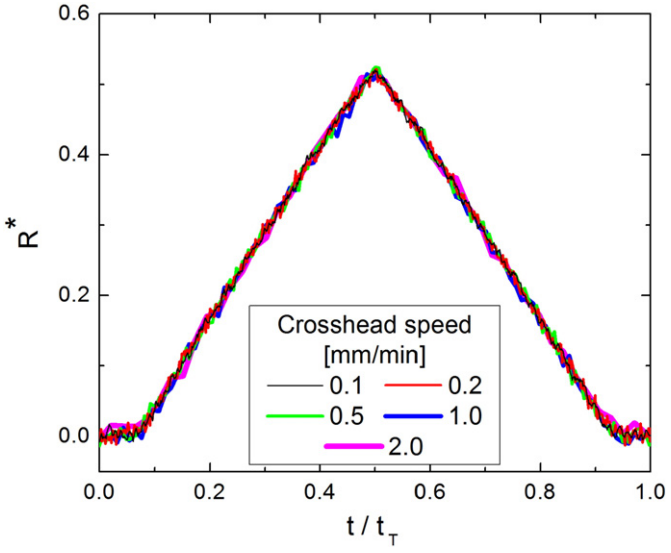

Fig. 8. The behavior of the dimensionless resistance R^* as a function of the normalized time of the experiment for different crosshead speeds at a temperature of 50 °C. Specimen A.

Differentiation of Eq. (6) allows writing the following expression for the slope $dR^*/d\varepsilon$

$$\frac{dR^*}{d\varepsilon} = \frac{1}{\varepsilon_{tr}}\left(\frac{R_M - R_A}{R_A}\right) \tag{8}$$

This equation suggests the possibility of determining the coupling between the variables R^* and ε through the measurement of the electrical resistance of the specimen in both fully austenitic and fully martensitic conditions as a function of temperature. The assessment of the temperature dependence of the strain ε_{tr} associated with the stress induced transformation is also required. The knowledge of all the mentioned parameters would allow obtaining an alternative estimation of the slope $dR^*/d\varepsilon$ that can be compared with the previous estimations included in Fig. 9c.

The determination of the electrical resistance of austenitic and martensitic phases was made by performing the following experiments. Starting with the specimens in austenite at a temperature of 80 °C, the electrical resistance was measured while the sample was cooled down into the martensitic state. Two cases were analyzed. In the first, specimen B was cooled down from 80 °C to −30 °C in the temperature chamber of the testing machine under load control maintaining a constant applied tensile force of 294 N (equivalently to an applied stress in

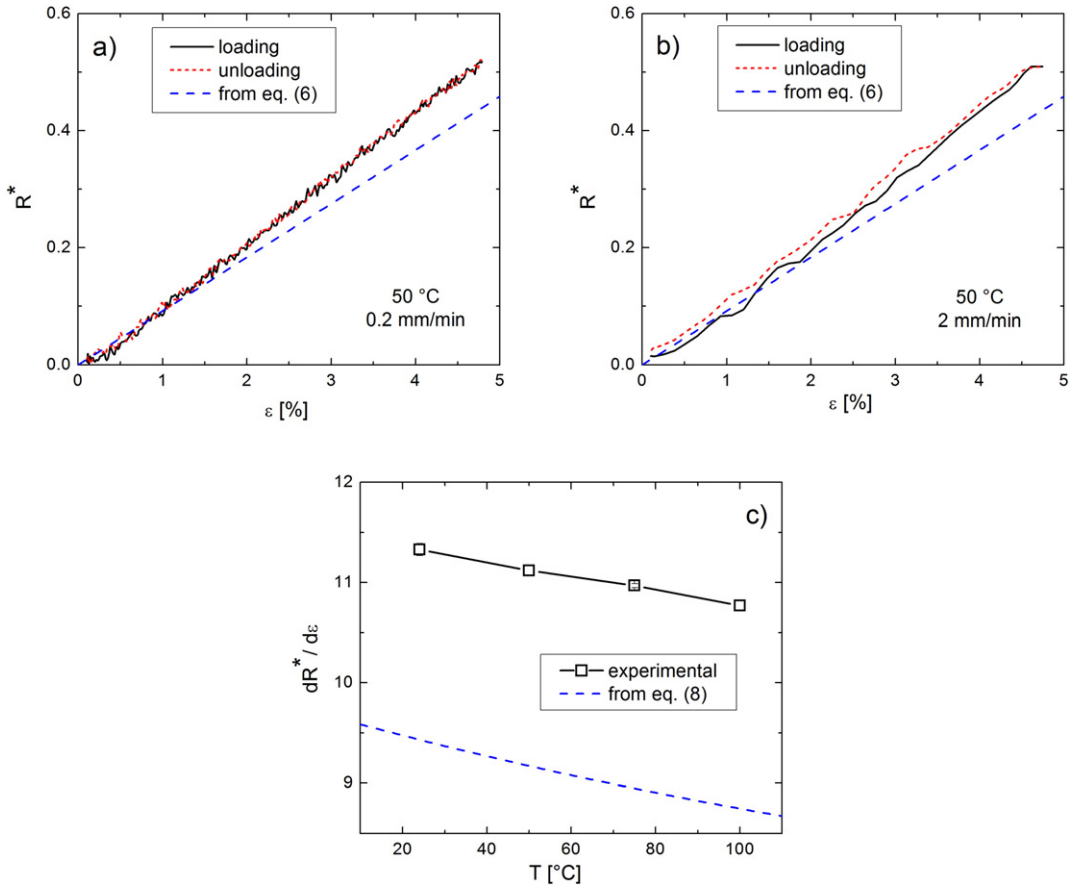

Fig. 9. Dimensionless electrical resistance R^* as a function of the transformation strain for experiments performed at 50 °C at a) 0.2 mm/min and b) 2 mm/min crosshead speed. c) Mean value of the slope $dR^*/d\varepsilon$ as a function of the temperature. The dashed lines represent an independent estimation of the corresponding functions using Eqs. (6) and (8). Specimen A.

austenite of 23 MPa). This procedure was made twice to check for repeatability. In the second case, the martensite was only thermally induced, i.e., no load was applied during cooling. A cooling rate of 3 °C/min was used in the experiments. In the first case a single-variant martensitic microstructure is expected, while the second corresponds to a multi-variant situation. Fig. 10 shows the corresponding evolution of the electrical resistance during cooling.

The occurrence of the transformation is clearly denoted in both cases by the abrupt increase of the electrical resistance at a certain temperature. In the high and low temperature extremes, the electrical resistance exhibits a linear dependence with temperature as expected for normal metallic materials. It is interesting to see that the load free and the under load experiments results in the same value of the electrical resistance in the temperature range where austenite is stable in both cases, i.e., above 40 °C. This is in line with the previous results mentioned when describing the weak effect of the applied stress on the electrical resistance change observed in the elastic range of the pseudoelastic cycle in Fig. 6. As expected from the dependence of critical stress with temperature shown in Fig. 3b (Clausius-Clapeyron), the transformation temperature is approximately 40 °C higher for the case where cooling was performed under load. It can also be seen that the electrical resistance corresponding to the multi-variant martensitic phase presents a lower value compared with the single-variant case. This constitutes a clear indication that the contribution of the interfaces to the electrical resistance in CuZnAl SMA is lower than the effect associated with the orientation of the single crystal. Based on the previous considerations, the temperature dependence of the electrical resistance of both phases were obtained by a least-square linear fitting procedure. A temperature interval from 0 °C to 80 °C was considered for austenite while an interval from −30 °C to 20 °C for martensite. The following expressions describe then the temperature dependence of the resistance of the specimen analyzed in the fully austenitic and fully martensitic conditions

$$\begin{aligned} RA &= (7.56 \pm 0.02)\ E{-}4\ T + (0.34502 \pm 0.00009) \\ R_M &= (9.32 \pm 0.01)\ E{-}4\ T + (0.60043 \pm 0.00002) \end{aligned} \tag{9}$$

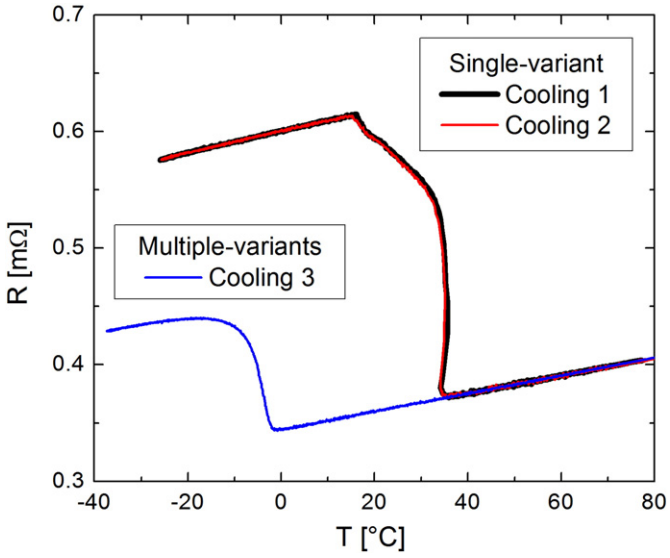

Fig. 10. Electrical resistance as a function of temperature, measured for three consecutive transformations from austenite to martensite. The first two cases under a constant load of 294 N (23 MPa) (single-variant experiments) and the last case without any load (multiple-variant experiment). Specimen B.

The temperature dependence of ε_{tr} is now assessed. Specimen B was used and a crosshead speed of 0.5 mm/min was selected for the experiments. The extensometer was used to evaluate the strain. Different working temperatures were used, following the sequence 25 °C, 55 °C, 85 °C, 40 °C, 70 °C and 100 °C. The curves corresponding to the transformation from austenite to martensite are shown in Fig. 11a. The elastic deformation of the austenite in all cases follow the same path until the transformation begins. From the crossover of this elastic slope and the corresponding critical transformation stresses it is possible to determine the initial strain (ε_{sta}) for each temperature. To determine the final strain (ε_{fin}), in Fig. 11b an enlarged view of the zone after the end of the transformation is presented, where it can be considered that the elastic loading of the martensite occurs (dotted rectangle in Fig. 11a). The strain ε_{fin} was determined by the intersection of the extrapolation of each of the martensitic elastic curves with the corresponding transformation plateaus. This allows determining the strain $\varepsilon_{tr} = \varepsilon_{fin} - \varepsilon_{sta}$ for the different temperatures that are plotted in Fig. 11c.

As these values were obtained using specimen B, they can be converted to values corresponding to specimen A through the respective Schmid factors. In that way, the following temperature dependence for ε_{tr} for specimen A is found

$$\varepsilon_{tr} = -(2.1 \pm 0.3)\, E{-}5\ \ T + (0.0763 \pm 0.0002) \tag{10}$$

The expressions given by Eqs. (9) and (10) are now used to calculate the value of R^* and $dR^*/d\varepsilon$ according to Eqs. (6) and (8). The resulting curves were drawn as dashed lines in Fig. 9. The comparison with the experimental points in Fig. 9c suggest a very similar sensitivity of $dR^*/d\varepsilon$ with temperature but with the absolute values differing around 22%. The origin of such discrepancy should be ascribed to the experimental uncertainties associated with the different variables involved and in particular with a possible dependence of the electrical resistance with crystal orientation in the material considered. Further work is required however to clarify these aspects.

The previous analysis constitutes, on the one hand, a clear example of the need of a proper determination of the characteristic parameters when modeling SMA for predicting complex transformation cycles, avoiding the use of the simplifications that could be assumed when relying in excess only in the equations. On the other hand, the temperature dependence of $dR^*/d\varepsilon$ works against the possibility of precise positioning by simply measuring the electrical resistance.

4.4. Influence of factors not considered by the model

There are two additional contributions to the electrical resistance that appear when changing the environmental conditions of the alloy, apart from the influence of the martensitic transformation. The first one is the elastic variation of the dimensions of the actuator due to the applied stress. The elastic deformation, denoted as ϵ to distinguish it from the transformation deformation, produces an increase in length and a decrease in cross-section, inducing a variation in the electrical resistance given by

$$R = R_0\, \frac{(1+\epsilon)}{(1-\nu\,\epsilon)^2} \tag{11}$$

being ν Poisson's ratio. Using typical values for $\epsilon = 0.003$ and $\nu = 0.33$ it results a maximum associated variation of the dimensionless resistance of $R^* = 0.005$, i.e., less than 100 times lower than the change associated with the full transformation.

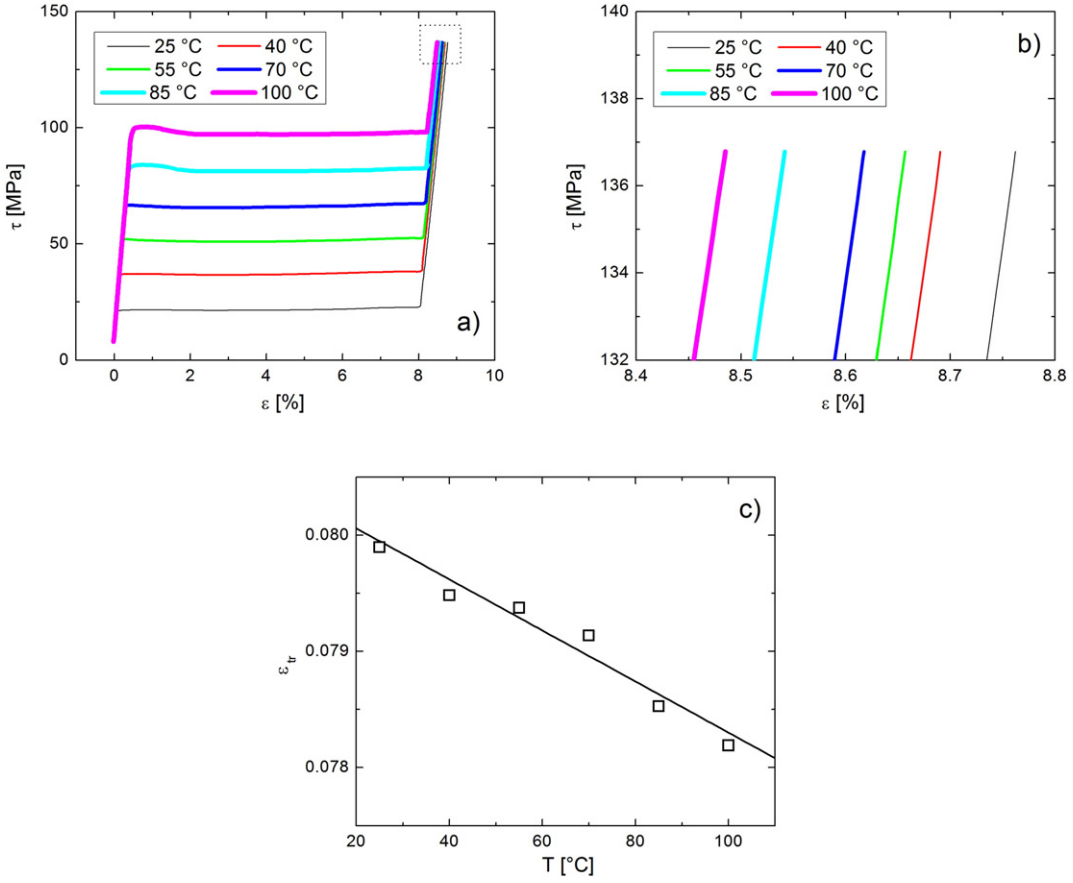

Fig. 11. a) Transformation branch of the pseudoelastic cycle for different temperatures. b) Detail of a), showing the elastic loading of the martensite. c) Transformation strain as a function of the temperature. Specimen B.

The second contribution arises from the thermal expansion of each of the phases which are subjected to temperature variations in a real application. In this case, both the specimen length and its area increase with a variation of temperature (ΔT). If α is the linear thermal expansion coefficient, the dimensionless resistance changes as

$$R^* = \frac{-\alpha\,\Delta T}{1+2\,\alpha\,\Delta T} \tag{12}$$

A variation of −0.002 is thus expected for a temperature increase of 100 °C in brasses.

Therefore, the contributions of both the elastic strain and the thermal expansion can be disregarded in comparison with the measured variations of R^* induced by the martensitic transformation. This is in line with all the experimental findings described before.

5. Conclusions

The analysis performed allows drawing the following important conclusions concerning the use of the electrical resistance for assessing the strain associated with the martensitic transformation in actuator positioning applications:

- The more significant qualitative aspects determining the relationship between strain and electrical resistance could be analyzed by a simple physics based model corresponding to the single variant transformation in a single crystalline CuZnAl shape memory alloy. A good qualitative correlation was observed between the model and the experimental behavior.
- The simple model developed here provides general guidelines for the selection and comparison of a shape memory material where the use of electrical resistance for positioning would give better results.
- Even in the simplest material case and uniaxial loading condition analyzed in the present work it was demonstrated that a precise correlation between strain and electrical resistance is limited. This can be even worse for other situations, i.e., materials with higher hysteresis (NiTi alloys for example) and complex dynamic conditions where the role of temperature would be more deleterious.
- Results suggest that the direct use of feedback from electrical resistance measurements for precise positioning is arguable unless particular quasi-static working conditions are assured.

Appendix A. Temperature dependent formulation

When considering possible variations of the temperature T, the basic model presented in Section 2 must be reformulated in the following way: Eqs. (1) and (5) read as follows

$$L(T) = (1-f)\,L_A(T) + f\,L_M(T) \tag{A1}$$

$$R(T) = (1-f)\,R_A(T) + f\,R_M(T) \tag{A2}$$

Both the length L_A as well as the corresponding resistance R_A, previously considered as the reference state, must be now defined at the reference temperature T_0. They will be denoted as $L_0 = L_A(T_0)$ and $R_0 = R_A(T_0)$. With these definitions it is possible to obtain an absolute deformation ε_0 and an absolute dimensionless resistance variable R_0^* in the form

$$\varepsilon_0 = \frac{[L(T)-L_0]}{L_0} = (\varepsilon+1)\frac{L_A(T)}{L_0} - 1 \tag{A3}$$

$$R_0^* = \frac{[R(T)-R_0]}{R_0} = (R^*+1)\frac{R_A(T)}{R_0} - 1 \tag{A4}$$

When analyzing the relationship between the resistance and the deformation using these just defined variables, it is easy to deduce from Eqs. (A3) and (A4) that the slope $dR_0^*/d\varepsilon_0$ is related to the isothermal slope presented in Eq. 8 by the expression

$$\frac{dR_0^*}{d\varepsilon_0} = \frac{R_A(T)}{R_0}\frac{L_0}{L_A(T)}\frac{dR^*}{d\varepsilon} \tag{A5}$$

As the thermal expansion coefficient is small, around 10^{-5} 1/K, the lengths ratio in Eq. (A5) can be disregarded and the only amendment to the slopes arises from the temperature dependence of the electrical resistance of the austenite.

References

[1] K. Otsuka, C. Wayman, Shape Memory Materials, Cambridge University Press, Cambridge, 1998.
[2] T.W. Duerig, K.N. Melton, D. Stockel, C.M. Wayman, Engineering Aspects of Shape Memory Alloys, first ed. Butterworth-Heinemann, London, 1990.
[3] P. Wollants, J.R. Roos, L. Delaey, Thermally and stress induced thermoelastic martensitic transformations in the reference frame of equilibrium thermodynamics, Prog. Mater. Sci. 37 (1993) 227–288.
[4] H. Yin, Y. He, Q. Sun, Effect of deformation frequency on temperature and stress oscillations in cyclic phase transition of NiTi shape memory alloy, J. Mech. Phys. Solids 67 (2014) 100–128.
[5] M. Ahlers, Martensite and equilibrium phases in Cu-Zn and Cu-Zn-Al alloys, Prog. Mater. Sci. 30 (1986) 135–186.
[6] H. Soul, A. Yawny, Thermomechanical model for evaluation of the superelastic response of NiTi shape memory alloys under dynamic conditions, Smart Mater. Struct. 22 (2013) 035017http://iopscience.iop.org/0964-1726/22/3/035017.
[7] J. Mohd Jani, M. Leary, A. Subic, M.A. Gibson, A review of shape memory alloy research, applications and opportunities, Mater. Des. 56 (2014) 1078–1113.
[8] W. Huang, On the selection of shape memory alloys for actuators, Mater. Des. 23 (2002) 11–19.
[9] D. Honma, Y. Miwa, N. Iguchi, Application of shape memory effect to digital control actuator, Bull. JSME 27 (1984) 1737–1742.
[10] C.J. De Araujo, M. Morin, G. Guénin, Electro-thermomechanical behaviour of a Ti-45.0Ni-5.0Cu (at.%) alloy during shape memory cycling, Mater. Sci. Eng. A 273–275 (1999) 305–309.
[11] P.-A. Gédouin, S.A. Chirani, S. Calloch, Phase proportioning in CuAlBe shape memory alloys during thermomechanical loadings using electric resistance variation, Int. J. Plast. 26 (2010) 258–272.
[12] E. López Cuéllar, G. Guénin, M. Morin, Study of the stress-assisted two-way memory effect of a Ti-Ni-Cu alloy using resistivity and thermoelectric power techniques, Mater. Sci. Eng. A 358 (2003) 350–355.
[13] K. Taillard, S. Arbab Chirani, S. Calloch, C. Lexcellent, Equivalent transformation strain and its relation with martensite volume fraction for isotropic and anisotropic shape memory alloys, Mech. Mater. 40 (2008) 151–170.
[14] M. Pozzi, G. Airoldi, The electrical transport properties of shape memory alloys, Mater. Sci. Eng. A 273-275 (1999) 300–304.
[15] X.D. Wu, J.S. Wu, Z. Wang, The variation of electrical resistance of near stoichiometric NiTi during thermo-mechanic procedures, Smart Mater. Struct. 8 (1999) 574–578.
[16] V. Novák, P. Sittner, G.N. Dayananda, F.M. Braz-Fernandes, K.K. Mahesh, Electric resistance variation of NiTi shape memory alloy wires in thermomechanical tests: experiments and simulation, Mater. Sci. Eng. A 481-482 (2008) 127–133.
[17] G.B. Stachowiak, P.G. McCormick, Shape memory behavior associated with the R and martensitic transformations in a NiTi alloy, Acta Metall. 36 (1988) 291–297.
[18] N. Ma, G. Song, H.-J. Lee, Position control of shape memory alloy actuators with internal electrical resistance feedback using neural networks, Smart Mater. Struct. 13 (2004) 777–783.
[19] B. Lynch, X.-X. Jiang, A. Ellery, F. Nitzsche, Characterization, modeling, and control of Ni-Ti shape memory alloy based on electrical resistance feedback, J. Intell. Mater. Syst. Struct. 1-19 (2016).
[20] H. Cho, T. Yamamoto, Y. Takeda, A. Suzuki, T. Sakuma, Exploitation of shape memory alloy actuator using resistance feedback control and its development, Prog. Nat. Sci.: Mater. Int. 20 (2010) 97–103.
[21] D. Cui, G. Song, H. Li, Modeling of the electrical resistance of shape memory alloy wires, Smart Mater. Struct. 19 (2010) 055019 (8pp).
[22] T.-M. Wang, Z.-Y. Shi, D. Liu, C. Ma, Z.-H. Zhang, An accurately controlled antagonistic shape memory alloy actuator with self-sensing, Sensors 12 (2012) 7682–7700.
[23] A. Caneiro, M. Chandrasekaran, Thermoelastic martensitic transformation in β Cu-Zn-Al studied by density changes, Scr. Metall. 22 (1988) 1797–1800.
[24] J. Olbricht, A. Yawny, J.L. Pelegrina, A. Dlouhy, G. Eggeler, On the stress-induced formation of R-phase in ultra-fine grained Ni-rich NiTi shape memory alloys, Metall. Mater. Trans. A 42 (2011) 2556–2574.
[25] J.L. Pelegrina, A. Yawny, J. Olbricht, G. Eggeler, Transformation activity in ultrafine grained pseudoelastic NiTi wires during small amplitude loading/unloading experiments, J. Alloys Compd. 651 (2015) 655–665.
[26] M. Ahlers, J.L. Pelegrina, Ageing of martensite: stabilisation and ferroelasticity in Cu-based shape memory alloys, Mater. Sci. Eng. A 356 (2003) 298–315.
[27] C.H. Gonzalez, M. Morin, G. Guénin, Behaviour of electrical resistivity in single crystals of Cu-Zn-Al and Cu-Al-Be under stress, J. Phys. IV France 11 (2001) (Pr8-167-172).